Single-shot, time-resolved planar laser-induced incandescence (TR-LII) for soot particle sizing – Part I: in a laminar flame

Z.W. Sun[1, 2, *], Z.T. Alwahabi[2, 3], G.J. Nathan[1, 2] and B. Dally[1, 2]
[1]School of Mechanical Engineering, University of Adelaide
[2]Center of Energy Technology, University of Adelaide
[3]School of Chemical Engineering, University of Adelaide

Abstract

Primary soot particle sizing by time-resolved laser-induced incandescence (TR-LII) imaging in a flat, laminar sooty C_2H_4/air flame is demonstrated in the present work. The primary soot size is determined by fitting the LII signals recorded by four subsequent images to the theoretical LII temporal decays relationship. A low laser power was chosen, to induce weak soot particle sublimations, in a laminar premixed sooty flame. A mean size of 13 nm was measured for the primary particles. This, and the size distributions of soot particles, is in good agreement with the time-resolved single-point-measurements and by sampling methods.

Keywords: soot, time-resolved, laser-induce incandescence, soot particle size, sooty flame

1. Introduction

Soot particles have a significant impact on the climate change and on human health, providing strong motivation to mitigate them. A recent study showed that the contribution of soot to global warming is much higher than initially estimated [1]. To understand the soot formation process and then perform reliable predication of soot particles in industrial furnaces, boilers and engines, accurate experimental data are required in well characterized ‘target’ flames suitable for model validation. Various nonintrusive laser-based techniques are applied in sooty flames to measure important parameters, for example, flame temperature by two-line laser-induced atomic fluorescence (TLAF), soot volume fraction and primary particle sizing by laser-induced incandescence (LII), soot aggregated sizes by wide angle light scattering [2]. Compared with particle-free flames, measurements using optical methods in sooty flames are more challenging, due to the presence of solid particles and high radiation [3], especially for planar measurements which are desirable in turbulent environments due to the additional spatial information they provide. Only the measurement of soot volume fraction using LII has been relatively well-developed. Optical methods for measuring the flame temperature, mixture fraction and soot particle (primary and aggregated) size are still highly under development. In particular, planar technique for the measurement of soot particle size has been rarely demonstrated.

The radius of primary soot particles (r_p) in flames has been widely measured in laminar flames by time-resolved LII (TR-LII) and two-color time-resolved LII (TC-TR-LII), but only on single-point. The only technique previously applied to turbulent conditions is the so-called ‘RAYLIX’ method [4], which simultaneously employs simultaneous LII and Rayleigh/Mie scattering. The value of the particle radius, r_p, is derived based on the assumption that LII signal scales closely with r_p^{3} while the scattering signal scales closely with r_p^{6}. In RAYLIX, the soot particles are assumed to be isolated and the scattering behaviour of soot aggregates is completely neglected, which is a questionable assumption [5]. Hence the aim of the present investigation is to extend TR-LII form single-point-measurement to two-dimensional (2D) imaging, to allow soot sizing to be performed on a planar sheet especially in turbulent sooty flames.

In LII, soot particles are heated by a short laser pulse with high radiation flux to a temperature far higher than the surrounding gases. Consequently, the near-blackbody radiation they emit is at a shorter wavelength than the background, generating a distinct incandescence signal that is proportional to the volume fraction of soot in the flame. Since large soot particles cool more slowly than small ones, the temporal history of the signal decay (normally in hundreds of nanoseconds) can be used to indicate soot particle size. Combining the measured temporal evolution of an LII signal and the theoretical thermal behavior of heated soot, the size of the primary particles can be derived. However, the accuracy of the measurements depends on the resolution of the temporal decay of the signal. This makes the measurement much more challenging in 2D as compared to the single-point method, due to the relatively low sensitivity of the imaging sensors (normally, intensified CCD cameras) and to the limited number of images that can be used to record the decay of a given pixel.

To attempt to meet this challenge, an ultra high speed camera system was employed to achieve time resolution in the order of nanoseconds, as is required to achieve TR-LII in 2D. This is combined with a model of the theoretical LII signal decay to allow a measurement to be performed from four images. The specified aims of the investigation are therefore to select the most suitable laser power for these 2D TR-LII measurements and to assess its accuracy in a well-characterised laminar flame.

* Corresponding author:
Phone: (+61) 8 83132310
Email: zhiwei.sun@adelaide.edu.au

2. Methodology

2.1 The LII model

Various LII models have been developed by different research groups. Schulz *et al.* summarized these models in a review paper [6]. All of these models solve the mass- and energy-balance equations for temperature and primary particle size, but adopt different approximation schemes for thermal conduction and different expressions for parameters such as the refractive index, E(m), and the thermal accommodation coefficient, α. In the present work, the model developed by Bladh *et al.* [7] is used to simulate the LII signals, providing a database with which to calculate particle size. This LII model has taken into the effect of soot aggregates and is being developed to include the fractional structure of the aggregates. Briefly, in the LII model by Bladh, the energy balance equation is written as

$$\dot{Q}_{\mathrm{abs}} - \dot{Q}_{\mathrm{cond}} - \dot{Q}_{\mathrm{sub}} - \dot{Q}_{\mathrm{rad}} = \dot{Q}_{\mathrm{int}} \ , \qquad (1)$$

where $\dot{Q}$ expresses the rate of change of a particle's energy generated respectively by absorbing laser power, by heat conduction, by sublimation, by radiation and the internal energy. The detailed expression and the related physical explanations for each term in equation *(1)* can be found elsewhere [7].

In the present work, soot aggregates are assumed to be composed of 100 primary particles, i.e., 100 primary particles per aggregate. Fuchs heat conduction model [8, 9] is used to handle the heat transfer from soot particles to surrounding gases, in which a soot aggregate is treated as an equivalent sphere. In simulation of the LII signals, a Log-normal function with a standard deviation of 0.2 is applied to characterize the size distribution for each mean particle diameter (d_p). The LII signal decay is a function of the ambient temperature. However, a constant temperature of 1700 K is assumed to simulate the LII signals. The LII model code is written using the MATLAB software. The intensity ratios of the LII signals from four cameras with a fixed delayed has direct relations to d_p. The modeling signal ratios are built in a look-up table to be used for fitting the measured ratios of LII signals to derive the value of d_p.

2.2 Determine particle size by LII signal decay

Two simulated LII signal decays of soot particles with different diameters are shown in Fig. 1. In contrast to TR-LII measurements obtained with single-point detectors, in the 2D TR-LII a series of two or more images are recorded after the laser pulse (as S_i shown in Fig. 1) at different delay times. Hence the local decay curve can be calculated for each pixel, $\tau(x, y)$, notably by fitting a pure exponential function to each series of LII signal intensities $S_i(x, y)$, where i = 1 to 4. However, the present investigation found that, because of the limited number of subsequent images, the approach of exponential fitting did not work well for some of the pixels. Alternatively, the ratio between two successive time-integrated LII signals are adopted to estimate the soot particle size, following earlier work [10]. As is also

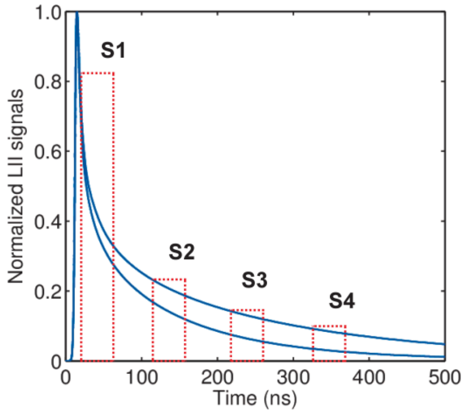

Figure 1 Schematic of time-resolved LII to determine the size of soot particles. The decay history of the heated soot particles can be reconstructed by consequently images. Emissions from soot particles of different sizes results in different ratios of S_2/S_1, S_3/S_1 and S_4/S_1. The soot particle sizes are fit from the comparisons between the measured values (i.e., S_2/S_1, S_3/S_1 and S_4/S_1) with the modeling results.

shown in Fig. 1, the ratios of S_2/S_1, S_3/S_1 and S_4/S_1 were fit to the modeling results to generate three values for the measured particle size. The mean value of these three values has been chosen to provide the final measure of the mean size of soot particles for each pixel.

The LII signal decay is a function not only of the particle size, but also of the initial temperature of particles to which particles are heated by the laser (and hence of the laser power). The particle initial temperature is typically used as an input parameter in soot sizing using TR-LII. Therefore, accurate determination of the particle temperature immediately or at a delay time after the laser pulse is essential in TR-LII for particle sizing. Two- or three- color pyrometry is typically employed in LII to determine the initial particle temperature. However, in the current work it was found that low accuracy was achieved for 2D pyrometry using the two band-pass filters centered at 430 nm and 525 nm, as shown later from Fig. 2b. Therefore, although it is generally agreed that a relative weak laser power should be applied to avoid soot sublimation in single-point LII [6], here a laser power that weakly induced soot sublimations was chosen to heat soot particles to their maximum temperature of around 4400 K [11].

3. Experimental arrangement

The fundamental output (1064 nm) from a Nd:YAG laser (Surlite II, Continuum) provided the laser source in LII measurements. The laser beam was firstly expanded by a telescope system (1:2) and the central portion (about half in diameter) was selected by an aperture to heat the soot particles. The round laser beam was reformed into a laser sheet by two cylinder lenses before being sent into the flame. The laser sheet in the imaged region is about ~ 15 mm in height and ~ 0.9 mm in thickness. The laser power was varied by a Glan-laser polarizer while maintaining the spatial and temporal profiles of the laser beam.

The LII signals were recorded by an ultra high speed camera (HSFC pro). LII signals were firstly split by an image splitter unit and then taken by four intensified

Table 2. Summary of optical filters and timing used for the HSFC Pro for the assessment of the influence of laser power**.**

Camera	Optical filters* (center/ bandwidth)	Time delay (ns)**	Integration time (ns)
1	430 nm / 60 nm	0	20
2	525 nm / 80 nm	100	40
3	525 nm / 80 nm	0	20

* With a near-Gaussian profile transmission.
** Relative to the start time of the laser pulse

CCD camera modules. The four images can be taken simultaneously or subsequently, controlled in nanosecond scale by the timing system of the camera. The HSFC camera and the laser were synchronized by using a digital delay/pulse generator (Stanford, DG535). Different optical filters can be put in front of each individual camera. The laser power used (see *section 4.1* for more details), the camera timing and the filters used are summarized in Table 1. In order to obtain a 2D soot sizing in a flat laminar flame (section 4.2), the four cameras are delayed at 0, 80, 160 and 240 ns relative to the starting time of the laser pulse. A band pass filter (510 - 590 nm) and an integration time of 30 ns were applied to all four cameras.

A water-cooled McKenna-type burner was used to produce a flat, laminar premixed C_2H_4/air sooty flame with an equivalence ratio of 2.0. The diameter of the central porous part is 30 mm. A steel plate of 20 mm thickness was positioned at 20 mm above the burner surface to stabilize the flame and prevent any flickering. No shielding co-flow was used.

4. Results and Discussion

4.1 Selection of the laser power

To select the optimum laser power, the dependences on the laser power of (1) LII signal intensity, (2) the initial temperature of particles and (3) the ratio of LII signals at two different delays on the laser power were investigated in a laminar C_2H_4/air (φ = 2.0) stabilized on a McKenna-type burner. Three cameras of the HSFC pro system were used and the experimental conditions are summarized in Table 1.

Figure 2 shows the results based on the statistics of 100 instantaneous images. All results were analyzed for an image area of 9.5 × 0.6 mm^2 (width × height, corresponding to 100 × 6 pixels^2) at a height of about 14 mm above the burner surface. As shown in Fig. 2a, the maximum of LII signal (from camera *3*) appeared at the laser power of 0.10 – 0.15 J/cm^2, above which the sublimation effect of soot particles resulted in weaker signals. A consistent trend is found in Fig. 2b. With increasing laser power below the peak (< 0.10 J/cm^2), the radiation of heated soot particles is blue-shifted due to the higher temperature. Above ~ 0.13 J/cm^2, the ratio of LII signals in the two spectral ranges (cameras *1* and *3*) behaved consistently, which indicates that the soot particles consistently reach the maximum achievable temperature, around 4400 K. Meanwhile, the LII signal

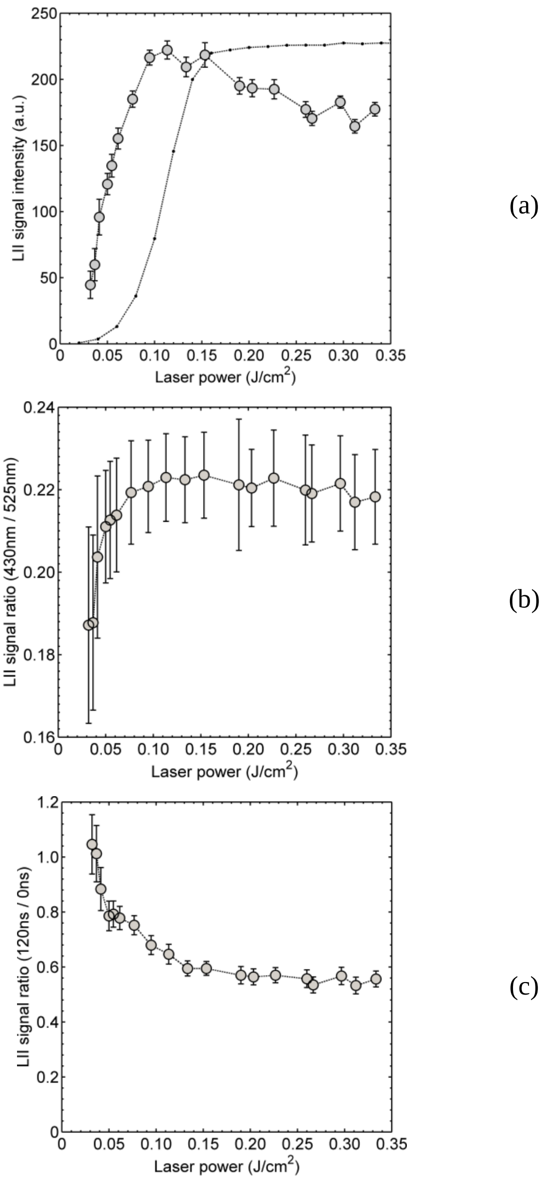

Figure 2 (a) the measured (*solid circles*) and modeled (*dark dots*) LII signal intensity, (b) the LII signal ratio between the two spectral ranges and (c) the LII signal ratio between two different delays as a function of the laser power. All results are from the statistics of 100 instantaneous images. The error bars are the standard deviation of these 100 images.

ratio between the two delay times (0 ns and 120 ns, i.e., the signals from cameras *2* and *3*) also approaches a constant value, as shown in Fig. 2c. This also indicates that the temperature of the heated soot particles is constant and that the particle size is not reduced significantly by the sublimation effect within the power range of 0.13 J/cm^2 to 0.35 J/cm^2. It should be noted that the sublimation effect influences the magnitude of the LII signals more strongly (Fig. 2a) than the soot particles' sizes (Fig. 2c). This can be explained by the fact that LII signals are proximately proportional to the cube of soot particles' sizes. Moreover, the large error bars in Fig. 2b indicate that there is a large uncertainty in determining soot temperatures using single-shot two-color pyrometry in 2D when using the current set of optical filters and even when averaging over an area of 100 × 6 pixels^2. Nevertheless, two-color TR-LII can still be attractive for

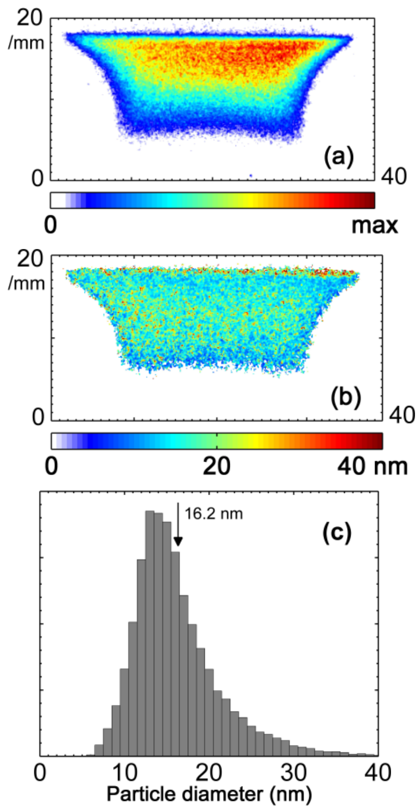

Figure 3 A typical instantaneous LII image (a) and its related image of soot particle sizes (b). The histogram of image (b) is shown in (c).

soot sizing if more suitable filters are used, for example, using filters centered at around 400 nm and 780 nm [12].

Therefore, a laser power of 0.13 J/cm^2 was chosen to image soot particle size for the rest of the experiments. Using this power, soot particles are weakly sublimated, while ensuring the heating of soot particles to ~ 4400 K, and hence minimizing the influence of unstable laser power on LII signals. It should be noted that in large turbulent flames the laser power is typically operated in the plateau region to avoid the influence of the attenuation of laser power induced by soot particles.

The dependence of the intensity of LII signals intensity on the laser power was also simulated with the model. By comparing the simulated and the measured curves as shown in Fig. 2a, a power of 0.20 J/cm^2 was chosen to simulate the signal decay curves as a function of the particle size, as in modeling soot particles are also weakly sublimated at this laser power.

4.2. 2D particle sizing in the laminar flame

A typical instantaneous LII image, together with the corresponding image of the size of primary soot particles, is shown in Fig. 3a and b, respectively, measured in the laminar flame. With an increase of in the height above the burner surface, the LII signal intensity (and hence the soot volume fraction) increased (Fig. 3a). The reason for the slight asymmetry in the LII image is unclear. The corresponding particle distribution, however, was much more homogenous as shown in Fig. 3b; only in the upstream (low position in Fig. 3b), the mean size of primary soot particle is relative small. The soot size measured here is in agreement with the observations by 2C-LII and transmission electron microscopy (TEM) [13]. Near to the surface of the steel stabilizer, a layer of the relative large particle sizes is found at the top of image in Fig. 3b, for which the explanation is still unresolved. The soot number density also increased with the height, which is a conclusion obtained by combining Fig. 3a and Fig. 3b.

Figure 3c shows the histogram of the measured values of d_p from across the entire image shown in Fig. 3b. A peak value of 13 nm as well as a mean value of 16.2 nm is obtained from the whole image in Fig. 3b. Worth noting, that an LII signal tends to be dominated by the large particles, which means that the small soot particles are underestimated using a TR-LII method. Moreover, from modeling LII signals it was found that the LII signal decay is only weakly sensitive to particle sizes above 50 nm, due to their relative small surface-to-volume ratio. Therefore, the uncertainty in the measurements obtained by TR-LII becomes larger for particles larger than 50 nm.

5. Conclusions

The planar measurement of the size of primary soot particles has been demonstrated using TR-LII in a laminar flat sooty flame, burning C_2H_4/air in a McKenna-type burner. The measurement is obtained from the average of three ratios, each of which was obtained from two successive LII images, separated by time-steps of tens of nanoseconds, requiring a total of 4 ICCD cameras. These ratios are used to determine the size of primary soot particles from a model of the LII decay curve, assuming a constant initial particle temperature. The optimum laser power was determined from the time-history of the LII signal intensity, the LII signal ratio between two spectral ranges and the LII signal ratio at two delay times. The image of soot particle size distribution in the McKenna-type burner was found to be in good agreement with published data obtained from single-point LII and TEM.

The accuracy of soot particles sizing using planar TR-LII depends particularly on the accuracy of the LII model used to simulate the signal decay, as is the case for single-point measurements. Similarly, the aggregation of soot particles is challenging to handle in all LII models, which results in significant uncertainty in primary soot particle sizing when using TR-LII. This suggests that a combination of TR-LII and elastic scattering techniques can be helpful to characterize soot particles size. Moreover, as expected, the LII decay curve also depends on the temperature of the surrounding gas phase media. Therefore, simultaneous TR-LII and a 2D thermometry (e.g. TLAF using Indium) will potentially improve the accuracy of TR-LII.

6. Acknowledgments

The Australian Research Council (ARC) is gratefully acknowledged for their funding support of this work and the current position of the first author.

7. References

[1]. T.C. Bond, S.J. Doherty, D.W. Fahey, P.M. Forster, T. Berntsen, B.J. DeAngelo, et al., Journal of Geophysical Research: Atmospheres **118** (11) (2013) 5380-5552.

[2]. P. Desgroux, X. Mercier and K.A. Thomson, P Combust Inst **34** (2013) 1713-1738.

[3]. G.J. Nathan, P.A.M. Kalt, Z.T. Alwahabi, B.B. Dally, P.R. Medwell and Q.N. Chan, Prog Energ Combust **38** (1) (2012) 41-61.

[4]. H. Geitlinger, T. Streibel, R. Suntz and H. Bockhorn, P Combust Inst **27** (1998) 1613-1621.

[5]. H. Oltmann, J. Reimann and S. Will, Appl Phys B-Lasers O **106** (1) (2012) 171-183.

[6]. C. Schulz, B.F. Kock, M. Hofmann, H. Michelsen, S. Will, B. Bougie, et al., Appl Phys B-Lasers O **83** (3) (2006) 333-354.

[7]. H. Bladh, J. Johnsson and P.E. Bengtsson, Appl Phys B-Lasers O **90** (1) (2008) 109-125.

[8]. A.V. Filippov and D.E. Rosner, Int J Heat Mass Tran **43** (1) (2000) 127-138.

[9]. F. Liu, K.J. Daun, D.R. Snelling and G.J. Smallwood, Appl Phys B-Lasers O **83** (3) (2006) 355-382.

[10]. S. Will, S. Schraml and A. Leipertz, Opt Lett **20** (22) (1995) 2342-2344.

[11]. F. Goulay, P. Schrader, X. López-Yglesias and H. Michelsen, Appl. Phys. B (2013) 10.1007/s00340-013-5504-4.

[12]. F. Liu, D.R. Snelling, K.A. Thomson and G.J. Smallwood, Appl Phys B-Lasers O **96** (4) (2009) 623-636.

[13]. H. Bladh, J. Johnsson, N.E. Olofsson, A. Bohlin and P.E. Bengtsson, P Combust Inst **33** (2011) 641-648.